How to cite: *Angew. Chem. Int. Ed.* **2022,** *61,* e202115778
International Edition: doi.org/10.1002/anie.202115778
German Edition: doi.org/10.1002/ange.202115778

Materials Chemistry | Hot Paper

The Orbital Origins of Chemical Bonding in Ge–Sb–Te Phase-Change Materials**

*Jan Hempelmann[+], Peter C. Müller[+], Christina Ertural, and Richard Dronskowski**

Abstract: Layered phase-change materials in the Ge–Sb–Te system are widely used in data storage and are the subject of intense research to understand the quantum-chemical origin of their unique properties. To uncover the nature of the underlying periodic wavefunction, we have studied the interacting atomic orbitals including their phases by means of crystal orbital bond index and fragment crystal orbital analysis. In full accord with findings based on projected force constants, we demonstrate the role of multicenter bonding along straight atomic connectivities. While the resulting multicenter bonding resembles three-center-four-electron bonding in molecules, its solid-state manifestation leads to distinct long-range consequences, thus serving to contextualize the material properties usually termed "metavalent". Eventually we suggest multicenter bonding to be the origin of their astonishing bond-breaking and phase-change behavior, as well as the too small "van-der-Waals" gaps between individual layers.

Introduction

Phase-change materials (PCM) have been an intensely discussed research subject for at least six decades.[1] Due to their unusual ability to quickly and reversibly switch between an amorphous and a physically distinguishable crystalline state, PCM find application in both *optical* and *resistive* memory storage devices in which the two phases are used to write and read the data.[2] Representatives of this material class are commonly found to comprise those compounds that violate the 8−*N* rule by a certain electron surplus, with main-group IV monotellurides such as GeTe, SnTe or PbTe being prototypical; note that the corresponding electron-precise 8−*N* representatives CaTe, SrTe, and BaTe (with noble-gas configurations for all atoms) behave unremarkably. Despite almost insignificant electronegativity differences,[3] the rocksalt type and related structures—usually found in ionic compounds—are common for GeTe, SnTe, and PbTe for which tetrahedral coordination (with shorter bond lengths needed for covalent bonding) would look more typical, at least at first sight.[4]

Given the set of unusual physical characteristics alluded to before and the significance of PCM for material science, it is hardly surprising that categorizing existing PCM and the search for even better ones has been the subject of vigorous research. Today, the sum of all empirical knowledge has allowed to frame a unique set of properties, often referred to as their *property portfolio*,[5] which typically includes[6] an extraordinarily large optical dielectric constant, an unusually large electrical conductivity, and a large Grüneisen parameter.[7] From a more chemical point of view, the high probability for multiple emission events in atom-probe tomography (APT)[8] is worth mentioning, so far interpreted as atoms "sticking together" even after having been ripped out from the bulk. The most obvious and indisputable structural property is given by the too small van-der-Waals gaps in layered PCM systems which refuses a convincing explanation until today.[9]

The aforementioned property set has proven to be an apt identifier for phase-change behavior although its origins have so far eluded an in-depth bonding analysis based on orbitals. Nonetheless, it has been possible to empirically *map*[10] various materials including PCM based on an electron-density partitioning scheme and thus derived descriptors for *ionicity* (electrons transferred, ET) and *covalency* (electrons shared, ES), thereby identifying prominent PCM as being positioned between the *covalent* and *metallic* bonding regimes. Ionicity seems to be negligible with near-zero electronegativity differences[3] which is reflected in small values of Mulliken and Löwdin charge for the respective atoms.[11,12] Consequently, the *metavalent bonding* term looks fitting for a region between (and also different from) metals and prototypical covalent materials.

[*] J. Hempelmann,[+] P. C. Müller,[+] C. Ertural, Prof. Dr. R. Dronskowski
Institute of Inorganic Chemistry, RWTH Aachen University
Landoltweg 1, 52056 Aachen (Germany)
E-mail: drons@HAL9000.ac.rwth-aachen.de
Prof. Dr. R. Dronskowski
Jülich-Aachen Research Alliance (JARA-CSD)
RWTH Aachen University
52056 Aachen (Germany)
and
Hoffmann Institute of Advanced Materials
Shenzhen Polytechnic
7098 Liuxian Blvd, Nanshan District, Shenzhen 518055 (China)
[+] These authors contributed equally to this work.

[**] A previous version of this manuscript has been deposited on a preprint server (https://doi.org/10.33774/chemrxiv-2021-6x89w).

In what follows, we will provide quantum-chemical evidence, by an orbital-based analysis of the underlying PCM wavefunction, that the mechanistic cause of *metavalent* bonding is the solid-state analog of *multicenter* bonding known from molecules violating the 8–*N* rule. The multicenter-bonding idea in the PCM context has recently been suspected,[13] and multicenter bonding occurring in Zintl–Klemm-like polyanions of Sb, Te, and Sn have been analyzed more than two decades ago.[14] Polyanions of that sort are entirely missing in the present (rocksalt-like) case, however, and we will evidence the electron-rich *cations* as being the source of multicenter bonding.

This study complements a previous theoretical PCM-related discovery, in particular the occurrence of unique long-range projected force constants pFC,[15] detected in rocksalt-type chalcogenide PCM.[11] In the spirit of a molecular quantum-chemical approach, we apply crystal orbital bond index (COBI) analysis to detect pairwise but also *multicenter* interactions, previously inaccessible for solids,[16] to be compared with fragment crystal orbital (FCO) decomposition.[17] Eventually, both COBI/FCO as well as pFC strongly suggest the same bonding situation when applied to the relevant GeTe–Sb_2Te_3 (often dubbed "GST") pseudobinary system.

In its various compositions, the GST system is among the most prominent phase-change materials in use today.[18] It is intimately related to Sb_2Te_3 (Figure 1) which crystallizes in the layered rocksalt-derived Bi_2Te_3-type,[19] with bond angles close to 90° and almost equal Sb–Te bond lengths but separated into five-atom thick "quintuple" layers (Te–Sb–Te–Sb–Te). Sb_2Te_3 can also be chemically "expanded" into the entire GST material family (Figure 1) with compounds such as $Ge_1Sb_2Te_4$ (GST124), $Ge_2Sb_2Te_5$ (GST225) and $Ge_3Sb_2Te_6$ (GST326). In their most stable structural variant, Ge is inserted in the center of the quintuple layer, effectively increasing the layer thickness by two atoms for each GeTe formula unit added.[20] Naturally, the more GeTe is added, the more the resulting phase approaches pure GeTe which crystallizes in the stable Peierls-distorted α-GeTe as well as the metastable rocksalt-type β-GeTe structure.[21] The somewhat mysterious structural gap *between* two layers (that is, between the terminal Te atoms) has often been referred to as a van-der-Waals (vdW) gap, for obvious reasons, but a closer look reveals that this gap is *significantly* (12 %) smaller than the sum of the vdW radii.[9] Because there is no external pressure in the GPa range, there *must* be more than simple vdW forces; indeed, previous projected COHP analysis has already detected small but significant covalency across the gap.[12] The latter stems from multicenter bonding, as elaborated below, present in the entire set of phase-change materials studied here.

As ingeniously recognized in 1927 already[22] by means of valence-bond theory, covalent bonding is a quantum-chemical *interference phenomenon* in which the interacting atomic wavefunctions (but not the electron density) interact either constructively (bonding) or destructively (antibonding), with all consequences for the resulting molecular wavefunction and its energetics. In modern molecular-orbital language,[23] the hydrogen molecule H_2 then results from two 1s atomic

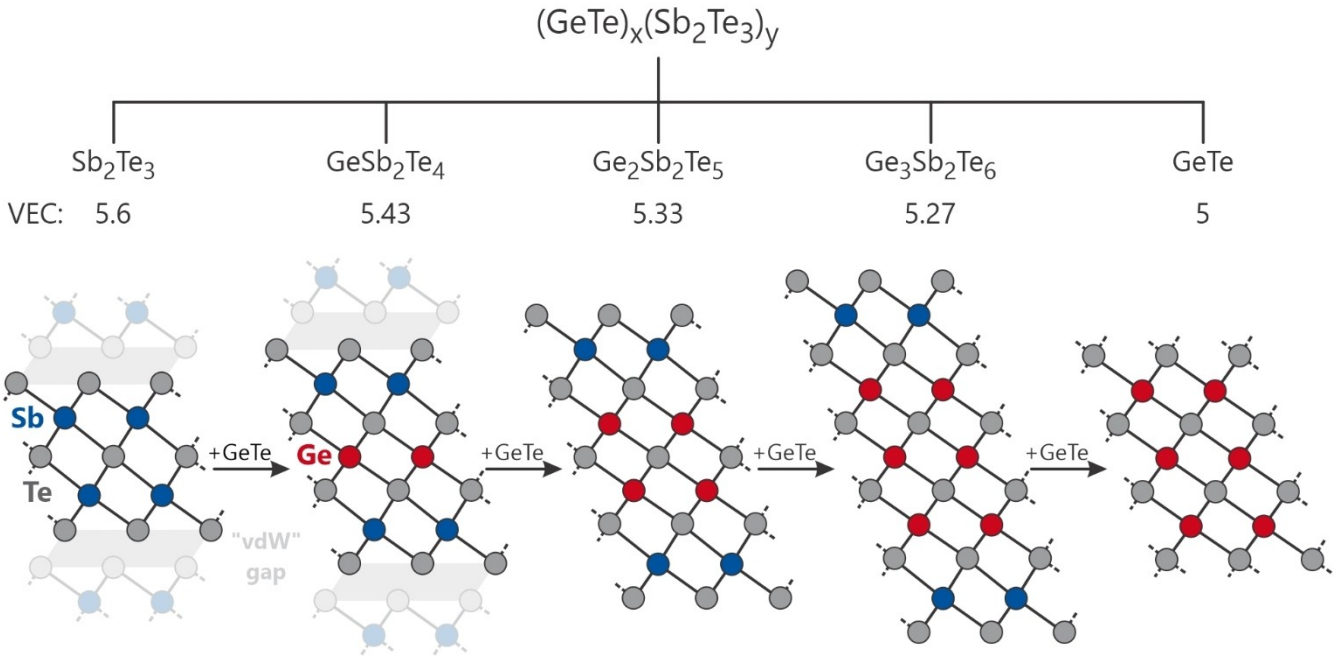

Figure 1. Schematic structural evolution of the GeTe–Sb_2Te_3 ("GST") pseudo-binary system shown as two-dimensional projections; starting from Sb_2Te_3 on the left, GeTe units are inserted in its very center. For Sb_2Te_3 and $GeSb_2Te_4$ on the left, the next two atoms of the adjacent layers (faded out) illustrate the position of the van-der-Waals gap. The end member on the right is rocksalt GeTe which does not possess such a gap. The valence-electron concentration (=total valence-electron count divided by the number of atoms) lowers from left to right: 5.6, 5.43, 5.33, 5.27, and 5.

orbitals constructively overlapping to give the bonding σ_g molecular orbital in which the two electrons are "stored" and yield an H–H single bond as well as the He noble-gas configuration for both H atoms; the antibonding σ_u* molecular orbital stays unoccupied, as sketched in Figure 2a,b by a DOS and COBI plot.[24] Essentially the same orbital-wise mechanism (only slightly more complicated due to more atomic orbitals) is found for diatomics such as N_2, larger molecules such as C_2H_6, and even for proteins of any size, all of them fulfilling the octet ($8-N$) rule. In case the latter rule is *not* fulfilled, *multicenter* bonding sets in, as has been established in molecular quantum chemistry for decades already, be it electron-deficient 3-center-2-electron (3c2e) bonds in B_2H_6[25] or electron-rich 3-center-4-electron (3c4e) bonds in XeF_2;[26] other scenarios have also been reported.[27] For the case of XeF_2, its electronic structure has also been sketched in Figure 2c–e. The existence of XeF_2 is due to σ-type molecular orbitals formed by the p-orbitals along the bonding direction[26c] but which also include an s-orbital contribution.[28] Despite Xe in XeF_2 having a valence electron count of 10 instead of 8, the final molecular orbitals are energetically lowered compared to the atomic orbitals, and there results a bonding interaction and a stable molecule. A detailed and even quantitative analysis of this bonding mechanism can be carried out by means of a generalized bond index for molecules[29] resembling the original Wiberg–Mayer idea.[30] The new crystal orbital bond index (COBI)[16] depicted in Figure 2 for molecular H_2 and XeF_2 not only serves as the periodic (solid-state) Wiberg–Mayer equivalent, it also allows to analyze three-center (four-center, five-center, etc.) in addition to pairwise interactions in both molecules and solids. For example, the three-center $COBI^{(3)}$ [cf. Equation (1)] is formed as an averaged product of density matrices involving atomic orbitals (μ, ν, χ) on three atoms and all their combinations.[16]

$$\mathrm{COBI}^{(3)} = P_{\mu\nu}P_{\nu\chi}\sum_{j,\mathbf{k}} w_{\mathbf{k}}\mathrm{Re}(c_{\chi j\mathbf{k}}{}^{*}c_{\mu,j\mathbf{k}})\cdot\delta(\varepsilon_j(\mathbf{k})-E) \quad (1)$$

The solid-state calculus is performed for all bands j at all $\mathbf{k}$. While the two-center COBI is quite intuitive as it translates to the chemical bond order, interpreting a multi-center bonding indicator is non-trivial. From molecular applications, it is well-known that negative numbers for the three-center bond index are found for electron-rich interactions while positive values are found for systems with an electron deficit. Hence, Figure 2d indicates a 0.49 two-center bond order for Xe–F based on the integrated $COBI^{(2)}$ (ICOBI) value, in addition to a significant −0.32 three-center F–Xe–F integrated $COBI^{(3)}$, thereby highlighting the multicenter bonding in XeF_2. In addition to two- and three-center interactions, there are also nonbonding contributions (black energy levels in the DOS plot in Figure 2c); we reiterate that such distinction between bonding, antibonding, and nonbonding is only possible through the orbital-phase information. All nonbonding contributions are given in red and illustrated by orbitals sketches, to be compared with Figure 2d,e. COBI in all its variants is part of LOBSTER[31] which allows for chemical-bonding analysis within a local-orbital framework but based on plane wave simulations.

Results and Discussion

For reasons that will become obvious in what follows, we first revisit rocksalt-type GeTe for which evidence for multicenter interactions has already been demonstrated, but via projected force constants,[11] that is, from the phononic point of view. Electronically, there have *also* been indications for multicenter bonding, indirectly so. An earlier COHP bonding analysis in Ge-defect rocksalt-type GeTe already showed that an intermediate Ge atom between two Te atoms leads to an *increase* of the Te–Te bond energy

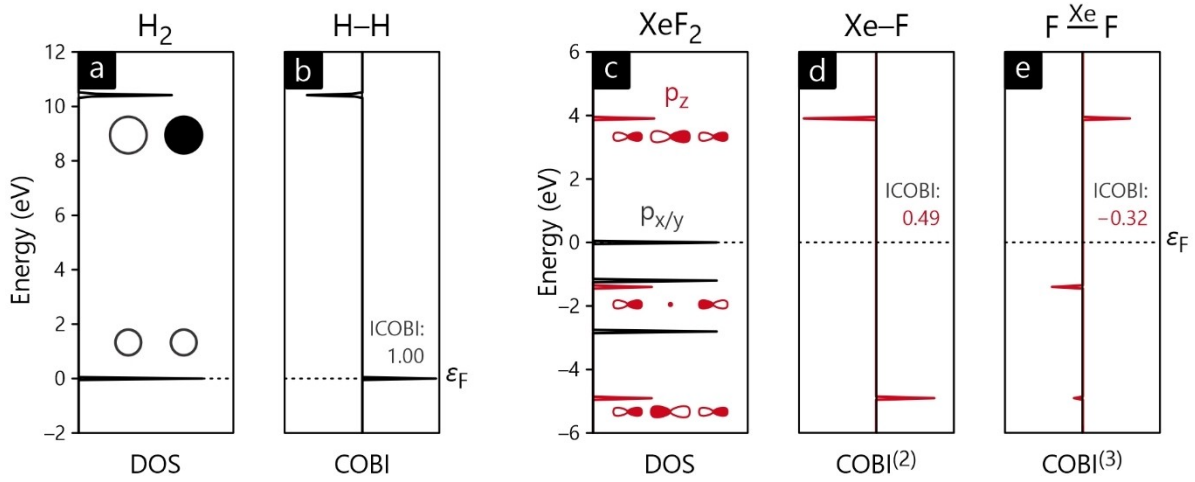

Figure 2. Molecular density of states (DOS) and crystal orbital bond index (COBI) plots for H_2 (a,b), as well as DOS, and two-center and three-center COBI plots for XeF_2 (c–e). The molecular DFT calculations were carried out using periodic boundary conditions and plane waves (VASP), eventually projected to local atomic orbitals for final analysis (LOBSTER).

(Kohn–Sham part) by a factor of almost 40; without the in-between Ge atom, there is almost no Te–Te interaction, so some kind of multicenter interactions *must* be present.[32] For simplicity, we will now focus on three-center interactions. Fortunately, due to the rocksalt type's high symmetry and p-orbital orthogonality, there are only two different kinds of three-center interactions to consider: one that spans from Te to Te, mediated by Ge, conveniently written as $Te\overset{Ge}{—}Te$ in our notation. Inversely, there is another one that spans from Ge to Ge and is mediated by Te; we formulate this as $Ge\overset{Te}{—}Ge$. For visual analysis, orbital-wise three-center COBI plots, their integrated values and how they combine for the total three-center interaction are depicted in Figure 3. Because there is no clear separation of molecule-like units in β-GeTe (unlike α-GeTe), assuming that such three-center bonds exist as discrete entities seems unfitting. Likewise, the interaction range is not necessarily limited to three centers, so we are likely looking at *partial* contributions to the total multicenter interaction across *n* centers as suggested previously.[11] The data were generated from density-functional theory (VASP),[33] projector-augmented waves,[34] the GGA-like PBEsol functional,[35] and a D3-correction with Becke–Johnson damping.[36] Monkhorst–Pack[37] **k**-point meshes and Brillouin-zone integration by Blöchl's tetrahedron method were used in reciprocal space.[38] When structurally optimized, the plane waves were projected onto a local-orbital basis using LOBSTER.[31,39] Quite obvious to the naked eye, the COBI plots in Figure 3 are qualitatively similar to each another, showing substantial orbital interaction across the same energy range. $p_x\overset{p_x}{—}p_x$ (Figure 3a,e) was already suggested as the main component to multicenter bonding, as confirmed by $COBI^{(3)}$ but $s\overset{p_x}{—}p_x$ also makes significant contributions. Notably, for $Te\overset{Ge}{—}Te$ the two orbital contributions add up to a net ICOBI of −0.10, whereas the ones for $Ge\overset{Te}{—}Ge$ compensate each other to yield a zero ICOBI value. That is to say that the in-between Ge atom (with a filled $4s^2$ configuration, locally deviating from the octet rule) is mediating the multicenter bond but in-between Te (with a formal Xe configuration, octet rule fulfilled) does not amount to a net bonding interaction. As such, the result is not too surprising but the simplified fragment crystal orbital (FCO) diagrams on the right (Figure 3d,h) further elucidate the bonding situation. In contrast to $COBI^{(3)}$ inherently describing the three-atom

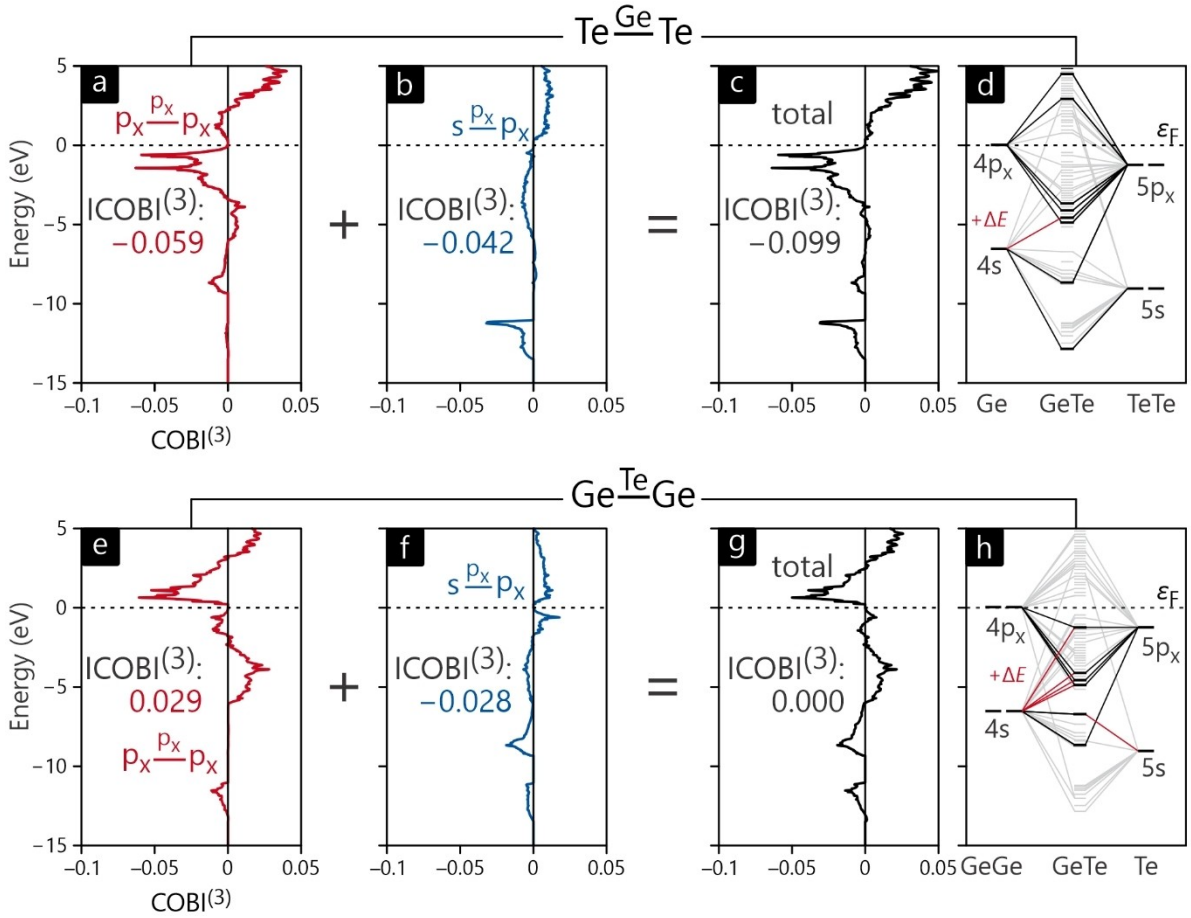

Figure 3. Orbital-wise and total three-center COBI plots for $Te\overset{Ge}{—}Te$ (a–c) and $Ge\overset{Te}{—}Ge$ (e–g) as well as their respective fragment crystal orbital (FCO) diagrams (d) and (h). The corresponding integrated ICOBI values are given. Note that for $Te\overset{Ge}{—}Te$, the $p_x\overset{p_x}{—}p_x$ and $s\overset{p_x}{—}p_x$ contributions add up to a total negative three-center ICOBI of approximately −0.10, while in $Ge\overset{Te}{—}Ge$ they annihilate each other (ICOBI = 0.00), indicative of a nonbonding state existing across several centers.

unit as one entity, the FCO analysis resembles a classic MO-like approach describing pairwise interactions as in a fragment molecular orbital diagram.[40] To keep interpretation simple for the extended solid, however, we model the TeTe fragment by two individual Te atoms which avoids another diagonalization of the respective Hamiltonian. Reiterating the FCO, the entire set of orbital interactions is represented as resulting from two interacting fragments (Ge and TeTe in Figure 3d).

Figure 3d,h reveal that there is significant orbital overlap, the individual 4s/4p and 5s/5p levels being very close in energy, thereby rationalizing the insignificant amount of charge transfer mentioned before; these are truly non-ionic materials.

For the Ge-mediated interaction in Figure 3a–d, the negative ICOBI may be understood just like multicenter bonding for molecules. GeTe with a valence-electron concentration of 5 (not 4 as for the $8-N$ equivalent CaTe) is an electron-*rich* system mediated by p-orbitals and therefore exhibits an electron-rich multicenter bond, manifesting in a negative ICOBI. Its value (−0.099) along *one* direction only is notably smaller than for the molecular case but this is to be expected: multicenter bonding occurs along *three* perpendicular directions and there may also be multicenter interactions with an even wider range beyond three centers. For molecular XeF_2, everything stops with the one-dimensional three-center case and $ICOBI^{(3)} = -0.32$.

For the $Ge\overset{Te}{-}Ge$ case, the peculiarities of periodic bulk materials become significant. Despite comparable degrees of orbital interaction below the Fermi level (evident by the non-zero values of the plots in Figure 3e,f), the $COBI^{(3)}$ integral amounts to a zero value (Figure 3g), as said before. By means of the fragment crystal orbital diagram, this very electronic state resembles a three-center equivalent of a *nonbonding* interaction. In molecular-orbital theory, nonbonding states may indicate the presence of lone-pairs, as they do in the classical case of the dinitrogen molecule.

While it is unlikely to be entirely analogous within the context of a three-center interaction—the degree of localization across the centers is unclear after all—the nature and existence of lone-pairs within the metavalently bonded family of materials has been vividly discussed in the past.[13,41] That is to say that the notion of a (directionally) partially delocalized "quasi lone-pair" as we may understand a three-center equivalent, is not unfounded.

Remarkably, while the two ICOBI values for $Te\overset{Ge}{-}Te$ and $Ge\overset{Te}{-}Ge$ are vastly different, the corresponding projected force constants (pFC) are almost the same, with the nonbonding three-center interaction even being larger in size. These lattice-dynamic properties were obtained with Phonopy,[42] the details given in the Supporting Information. We reiterate that pFC have been demonstrated to indicate multicenter interactions in GeTe.[11] While they rest on an entirely different theoretical background as regards forces and phonons, the resulting pFC easily quantify the *interaction strength* between any two atoms in a supercell. For the case of GeTe, extraordinarily strong force constants for atoms being very far apart suggested multicenter bonding as a possible explanation.

Coming back to the vanishing $Ge\overset{Te}{-}Ge$ three-center interaction, the electronic state is seemingly *nonbonding* in terms of orbital interactions (because they all cancel), resulting in no lowering of the energy for this state. And yet, the linear configuration is still so sensitive to geometric perturbation (resulting in a high pFC) that there is a *collective* net contribution of that nonbonding scenario which also supports the metastability of β-GeTe and the orthogonal linear chains facilitating multicenter $Te\overset{Ge}{-}Te$ interactions.

As an in-between summary, the $Te\overset{Ge}{-}Te$ and $Ge\overset{Te}{-}Ge$ examples illustrate how COBI and pFC complement each other in elucidating the bonding situation in materials like GeTe. We note that the two descriptors are entirely independent from each other and calculated from vastly different methodologies. While COBI (measuring the bond order) is extracted from the wavefunction, pFCs (measuring the bond stiffness) are derived perturbatively from atomic displacements. While the bond energy (as a measure of its "strength") and the corresponding force constant often run parallel to each other,[43] there is no obvious theoretical reason for them to be connected. For example, the bond dissociation energy of CO is higher than for N_2 but the opposite is true for the corresponding force constants. And yet, both descriptors appear to resolve the same physical phenomenon for PCM, albeit in a different manner. In a linear arrangement of p-orbitals, one may argue that the relationship of the phenomena detected by COBI and pFC is one of *cause* (linear multicenter orbital interaction) and *effect* (unusually high force constants between these far-off atoms), a consequence of the Born–Oppenheimer approximation, that is, the electronic structure preceding the vibrations.

If orbital-based COBI and lattice-dynamics-based pFC arguments are valid for multicenter bonding in rocksalt-type GeTe, they should also hold for other materials exhibiting the rocksalt motif given a similar valence-electron concentration. As alluded to before, such criteria also characterize prominent layered PCM like Sb_2Te_3 and the entire GST system, too. What will be the consequences of the limited chain length imposed by the terminal atoms (at the supposedly van-der-Waals gap) in these layered materials?

Figure 4 depicts the COBI plots and corresponding ICOBI values for different $Te\overset{M}{-}Te$ three-center interactions in various layered PCM as well as in rocksalt GeTe for comparison. Notably, as the GeTe content of the material increases and β-GeTe is approached, the ICOBI value *decreases* gradually from an initial −0.158 in Sb_2Te_3 to the previously discussed −0.099 for GeTe. Considering the chemical nature of GST as a pseudobinary system of Sb_2Te_3 and GeTe, this monotone shift is in line with chemical intuition because, as the Ge/Sb ratio increases, the valence-electron concentration decreases and, as a consequence, so does the ICOBI (bond order). While the additional GeTe units in the system lower the electron count, they do not appear to significantly change the underlying multicenter nature of chemical bonding; not too surprisingly, the projected force constants for these compounds remain large regardless of the GeTe content. Alternatively expressed,

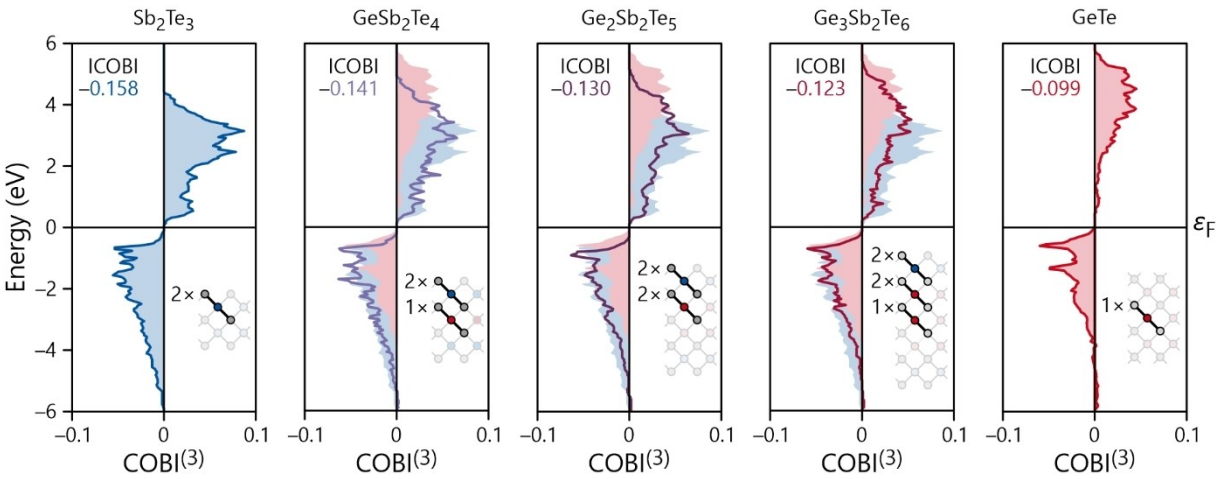

Figure 4. Averaged in-layer three-center Te$\overset{M}{-}$Te COBI for Sb_2Te_3, GST124, GST225, GST326 and GeTe. Note how the COBI gradually shifts from an Sb_2Te_3 (blue) to a GeTe (red) nature. The pictograms refer to the different kinds of three-center interaction present in the respective system.

atoms "sticking together" over large distances looks like a universal phenomenon in PCM and originates from multicenter bonding, and we reiterate that such behavior is well-known experimentally from atom-probe tomography.

Nonetheless, there is also a gradual change in overall shape of the electronic structures (visualized by the COBI plots in Figure 4) because the distinct Sb_2Te_3-like appearance steadily transforms to resemble the one of GeTe as more GeTe is introduced. That is to say that the GeTe content of the GST system appears to control the electronic properties of the compound,[44] but this effect does not fully translate into the chemical bonding mechanism.

And yet, the most remarkable discovery in probing the chemical-bonding nature of the layered Bi_2Te_3-type PCM is the occurrence of multicenter interactions—apparent from both COBI and pFC—bridging the supposedly van-der-Waals-like gap between individual layers.

As an illustrative example, we take the binary Sb_2Te_3 and its quintuple layers whose three- and four-center interactions are depicted in Figure 5; exactly the same phenomenon is found for the other members of the GST system as well. Besides obvious three-center interactions within the layer (as also highlighted before for bulk GeTe), there is also a significant degree of bonding interaction in the three-center Sb$\overset{\text{Te vdW}}{-}$Te (in red) *crossing the gap*, an electronic communication *between the layers* which is apparent both from a non-zero COBI plot as well as significant ICOBI of −0.041, about $^1/_4$ of the in-layer ICOBI. Similarly, the four-center Sb$\overset{\text{Te vdW Te}}{-}$Sb (also in red) shows a strikingly similar COBI behavior, its ICOBI value (−0.027) being almost as large as the three-center one, and it exhibits a force constant with a strength comparable to intralayer Te$\overset{\text{SbTe}}{-}$Sb, even stronger than the pFC for the three-center interaction across the gap. Evidently, multicenter interactions help maintaining the rocksalt structural motifs even *across* individual layers, and they provide an intuitive explanation as to the size of the gap between the layers. Multicenter orbital interactions make the gap shrink, significantly shorter than for regular van-der-Waals forces solely going back to vacuum fluctuations (and induced dipole-dipole interactions). Note that this has nothing to do with whatever *a posteriori* vdW correction to the exchange-correlation functional. Only here, such weak (but clearly stronger than vdW) Te–Te interactions across the gap remind us of the polyanionic interactions described in the literature, at least in terms of topology.[14a]

Mechanically, such gap-bridging interactions appear to differ slightly from those exclusively contained within a single layer, clearly visible in the smaller force constants and smaller ICOBI values for bridging interactions that end in a layer-terminating Te atom. This is likely connected to the break in the multicenter atomic *sequence* happening at the end of the layer, with two subsequent Te atoms instead of the usual alternation, resulting in an electronically different four-center interaction. There is significant electronic localization at the gap with evidence for the presence of lone-pairs,[41e] making the presence of the strong force constants and ICOBI even more unusual.

As presented before, upon going from the rocksalt type to layered compounds such as Sb_2Te_3, dismantling an extended structure's isotropy results in gradual changes as regards the multicenter bonding behavior which looks comparatively simple for the fundamental rocksalt systems. A detailed overview of the entire picture is given in Figure 6 in which projected force constants of multicenter interactions in a variety of compounds have been plotted against their corresponding integrated COBI values. Do these go together?

A glancing look at Figure 6a shows an apparent correlation between projected force constants (bond stiffness) and the crystal orbital bond index (bond order). Generally speaking, large force constant values correspond to a large (negative) multicenter ICOBI value, and vice versa. The figure also indicates, once again, that the bonding mechanism in the GST system does not qualitatively but only quantitatively change as the GeTe content increases. Irrespective of the actual composition, all equivalent multicenter indices and force constants are clustered together to

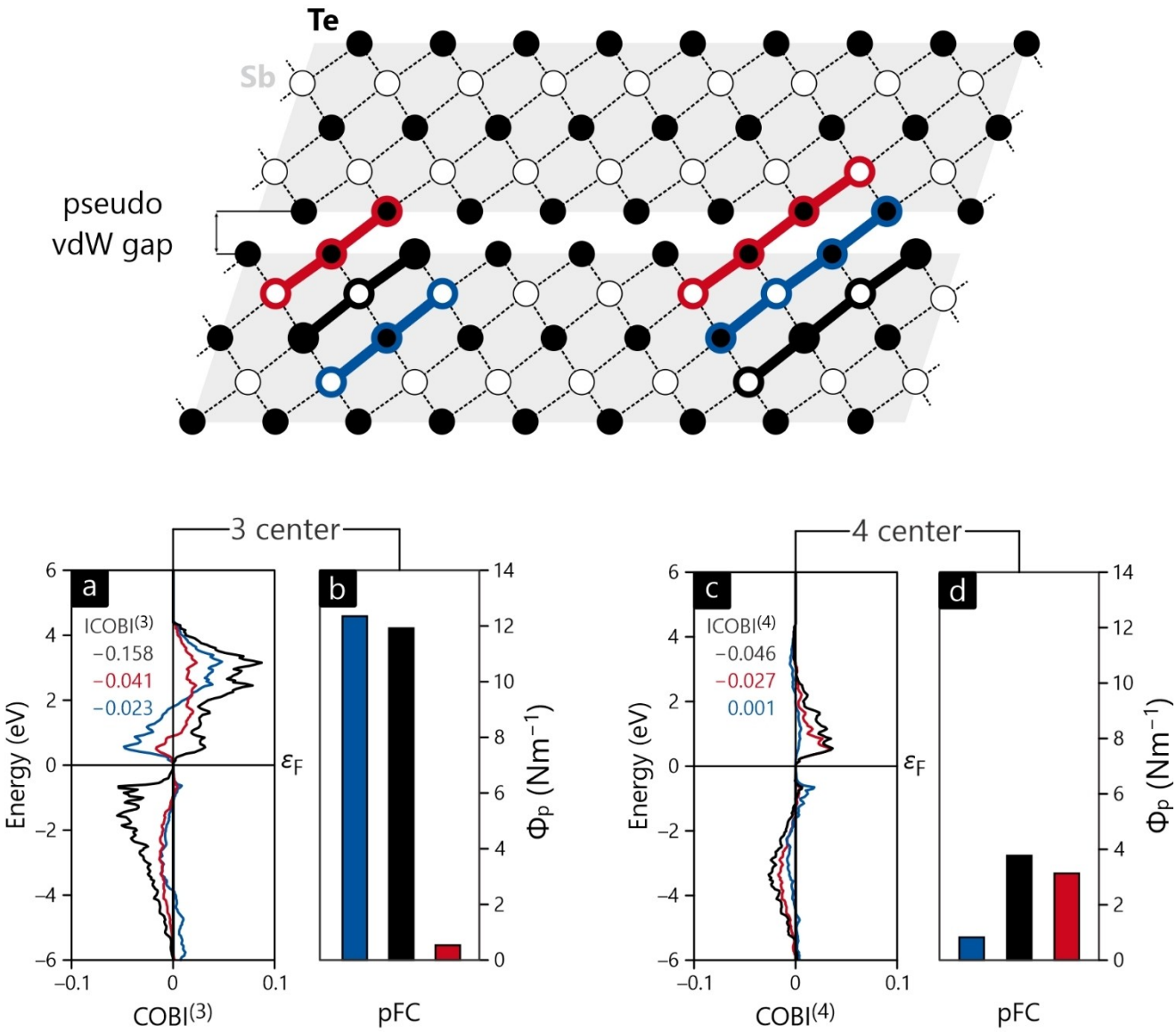

Figure 5. COBI plots (a,c) and projected force constants (b,d) for intra- and interlayer three- and four-center interactions in Sb_2Te_3. Note the significant values of both (I)COBI and pFC for the gap-bridging $Sb\overset{TeTe}{—}Sb$ four-center interaction.

such an extent that the attempt to make compositional differentiation seems difficult. Only the extreme system borders, that is, the binaries GeTe and Sb_2Te_3, are separated from the rest. This separation, however, is only observed in the projected force constant while the ICOBI values remain largely unchanged. As such, the difference in stiffness cannot originate from a difference in bonding mechanism.

Further, Figure 6b demonstrates that the ICOBI values of the different equivalent three-center interactions are a consequence of the *elemental nature* of the bridging atom involved in $Te\overset{Ge}{—}Te$, $Te\overset{Sb}{—}Te$ and $M\overset{Te}{—}M$, and all three of them form separate clusters with nearly identical ICOBI values; clearly, the bridging atom (and its local electron count) is decisive for the three-center bond order. For $M\overset{Te}{—}M$, this cluster at reference point (RP) 1 is located closely around ICOBI$\approx$0, largely independent of whether the precise motif is $Ge\overset{Te}{—}Sb$, $Ge\overset{Te}{—}Ge$ or $Sb\overset{Te}{—}Ge$, a single exception being $Sb\overset{Te}{—}Sb$ (appearing only in Sb_2Te_3) located comparatively far away at ICOBI$=-0.023$. We can safely conclude that these interactions involving a closed-shell atom (formally Te^{2-} with a noble-gas configuration) indicate an overall *nonbonding* state, as found before; even the outlier $Sb\overset{Te}{—}Sb$ with the highest 5.6 valence-electron concentration (lowest triangle in the bluish cloud) only slightly shifts into the bonding regime. Quite to the contrary, $Te\overset{Ge}{—}Te$ at RP 2 and $Te\overset{Sb}{—}Te$ at RP 3 are outstanding and significant three-center interactions, mirroring the role of electron-rich bridging atoms (formally Ge^{2+} and Sb^{3+} with a surplus of two electrons outside the noble-gas shell), and this is where most of the multicenter bonding originates, as also detailed before.

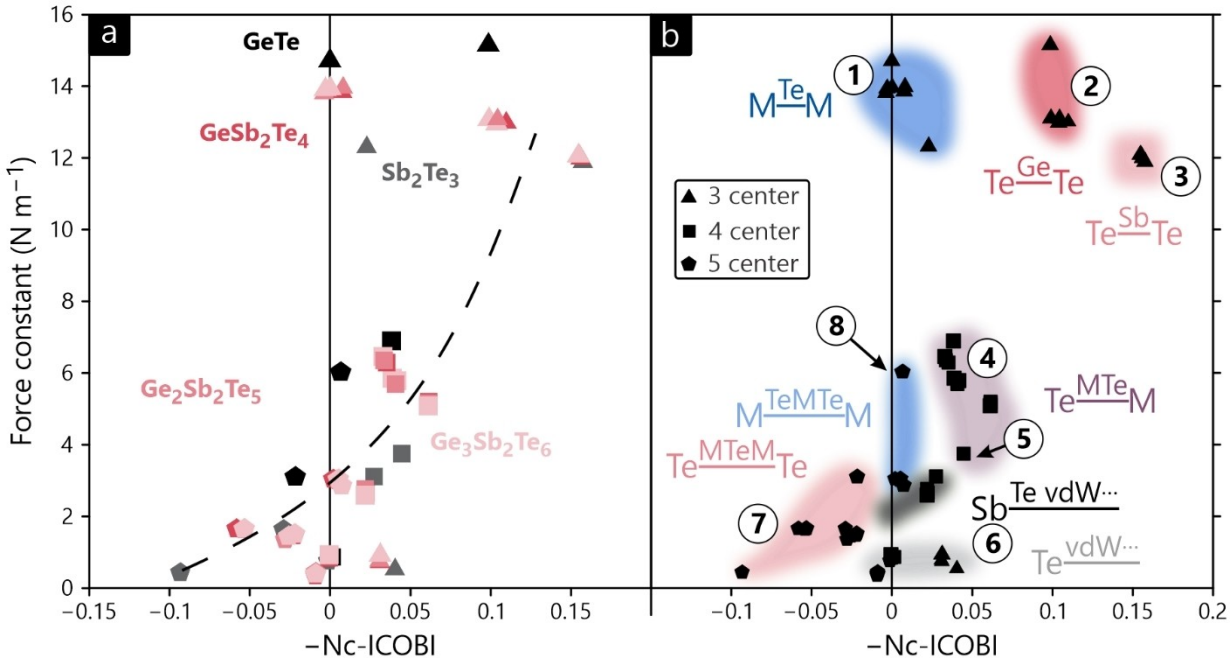

Figure 6. Projected force constants plotted against multicenter ICOBI for three-, four- and five-center interactions in GeTe, GST124, GST225, GST326 and Sb_2Te_3. In a) we show which data point belongs to which compound. In b), the data points are grouped according to the interaction type where M stands for either Sb or Ge, and vdW indicates an interlayer gap-bridging interaction. For better orientation, reference points such as ① have been sketched in b), please see text.

Intralayer four-center interactions also form a cluster with lowered ICOBI and pFC (RP 4), just as expected. Once again, Sb_2Te_3 (RP 5) appears as an outlier, exhibiting a far weaker pFC for its four-center interaction. The gap-bridging four- and five-center interactions (RP 6) which lead to too short van-der-Waals contacts have comparably strong force constants but approach ICOBI$\approx$0 already for five centers. In contrast, all multicenter interactions that include a chain-terminating Te atom have very small force constants and ICOBI.

Open questions remain, for example the occurrence of fairly weak five-center interactions with a *positive* ICOBI value (RP 7), yet to be explained. Even a simple chemical interpretation of such five-center index is challenging, as—to the best of our knowledge—no previous investigation of such a state has ever been tried. For a three-center case, positive values would indicate an electron-deficient multicenter bond but in the distinctly electron-rich systems investigated here, this is not a sensible interpretation. This is furthermore supported by their pFC which continue to fall and are the lowest for the largest positive ICOBI, which in turn is actually the most electron-rich compound Sb_2Te_3. We also note that some five-center interactions retain their negative ICOBI sign, with GeTe and its $Ge\overset{TeGeTe}{\text{—}}Ge$ interaction (RP 8) actually achieving force constants comparable to four-center interactions in the GST system. The range of the multicenter interaction could reasonably be interpreted as an indicator for the degree of electronic delocalization across the centers.

Conclusion

Given a tailored set of theoretical tools such as crystal orbital bond index and fragment crystal orbital analysis, an orbital-based study of the chemical bonding in the entire GST pseudobinary system has been carried out. In full accord with long-range projected force constants, there is clear evidence for electron-rich multicenter bonding for this class of compounds. To the best of our knowledge, such multicenter interactions mediated by electron-rich (formal) cations have never before been investigated, certainly not orbital-wise, for periodic solids, the simple reason being that the aforementioned tools were unavailable so far.

Both electronic-structure (COBI) and phononic-structure (pFC) descriptors support multicenter bonding primarily via electron-rich intermediate atoms such as Ge or Sb, to a smaller degree involving additional atoms, and even beyond van-der-Waals-like structural gaps. As such, the material properties portfolio usually related to metavalent bonding appear as a natural consequence of multicenter bonding, similar to the molecular case, but different due to the extended connectivity in the periodic solids. Not only does high delocalization across many centers naturally lead to an increased conductivity, the long-ranged forces between atoms "sticking together" as a consequence of multicenter bonding also serve as a simple explanation for the high probability of multiple emission events seen in atom-probe tomography. As alluded to before, structural gaps between layers are smaller than expected for van-der-Waals gaps, caused by the constructive atomic-orbital multicenter overlap between layers. In principle, such beyond-gap bonding

should be mirrored by an unusually high electron density within the gap, to be examined either theoretically by means of QTAIM[24] analysis or experimentally from high-resolution electron density maps.

Unsurprisingly, considering the thorough phenomenological description of metavalent materials, a multicenter bonding mechanism as presented here also characterizes this very bonding type as being akin to both metallic and conventional (two-center) covalent bonding, exhibiting both a delocalized but also a directed character. In fact, a similar classification of molecular electron-rich multicenter bonding bridging covalency and metallicity was also suggested in the context of an NBO analysis for Be–Li cluster models.[45] While covalent bonding results from the interference of wavefunctions, such a definition would strictly also include metallic bonding but one difference remains: although metallic bonding then appears as a special case of covalency, it is due to a *too small* number of electrons distributed over a plethora of atoms, hence completely delocalized across the bulk and therefore causing the characteristic metal properties.[46] Curiously, the likewise interfering wavefunctions with *too many* electrons as discussed in this work yield the aforementioned peculiar PCM properties. That is to say that electron-rich multicenter bonding—just like electron-poor metallic bonding—may be understood as a special case of covalency. Supported by the amount of theoretical and also experimental data, we therefore conclude that multicenter bonding is in good agreement with the property-based concept of metavalent bonding, and we suggest multicenter bonding as the actual quantum-chemical origin of metavalency.

As an outlook we suggest that the same strategy of combining the analysis of both wavefunction and lattice dynamics should also shed new light on the chemical bonding in other materials. For example, preliminary studies of ours on polyanionic compounds, regular Zintl phases, and also functional oxides such as high-temperature superconducting cuprates evidence unexpected, even astonishing behavior.

Acknowledgements

All authors gratefully acknowledge financial support obtained from Deutsche Forschungsgemeinschaft within SFB 917 “Nanoswitches”. Also, we thank the Jülich-Aachen Research Alliance (JARA) as well as RWTH Aachen University’s IT Center for having provided CPU time under project jara0033. Open Access funding enabled and organized by Projekt DEAL.

Conflict of Interest

The authors declare no conflict of interest.

Data Availability Statement

The data that support the findings of this study are available from the corresponding author upon reasonable request.

Keywords: Metavalent Bonding · Multicenter Bonding · Phase-Change Materials · Wavefunction Analysis

[1] a) M. Wuttig, N. Yamada, *Nat. Mater.* **2007**, *6*, 824–832; b) S. Raoux, *Annu. Rev. Mater. Res.* **2009**, *39*, 25–48; c) M. G. Kanatzidis, *Inorg. Chem.* **2017**, *56*, 3158–3173; d) C. Koch, G. Schienke, M. Paulsen, D. Meyer, M. Wimmer, H. Volker, M. Wuttig, W. Bensch, *Chem. Mater.* **2017**, *29*, 9320–9327.
[2] a) S. R. Ovshinsky, *Phys. Rev. Lett.* **1968**, *21*, 1450–1453; b) S. Raoux, W. Wełnic, D. Ielmini, *Chem. Rev.* **2010**, *110*, 240–267; c) S. Raoux, F. Xiong, M. Wuttig, E. Pop, *MRS Bull.* **2014**, *39*, 703–710; d) V. L. Deringer, R. Dronskowski, M. Wuttig, *Adv. Funct. Mater.* **2015**, *25*, 6343–6359.
[3] L. Pauling, *The Nature of the Chemical Bond*, Cornell University Press, Ithaca, NY, **1960**.
[4] E. Mooser, W. B. Pearson, *Acta Crystallogr.* **1959**, *12*, 1015–1022.
[5] B. J. Kooi, M. Wuttig, *Adv. Mater.* **2020**, *32*, 1908302.
[6] a) M. Wuttig, V. L. Deringer, X. Gonze, C. Bichara, J.-Y. Raty, *Adv. Mater.* **2018**, *30*, 1803777; b) Y. Cheng, S. Wahl, M. Wuttig, *Phys. Status Solidi RRL* **2021**, *15*, 2000482.
[7] The socalled Grüneisen parameter describes how the phonon frequencies depend on the volume, and it therefore serves as a measure of the anharmonicity of the lattice vibrations: E. Grüneisen, *Ann. Phys.* **1912**, *344*, 257–306.
[8] M. Zhu, O. Cojocaru-Mirédin, A. M. Mio, J. Keutgen, M. Küpers, Y. Yu, J.-Y. Cho, R. Dronskowski, M. Wuttig, *Adv. Mater.* **2018**, *30*, 1706735.
[9] M. Küpers, R. P. Stoffel, B. Bong, M. G. Herrmann, Z. Li, A. Meledin, J. Mayer, K. Friese, R. Dronskowski, *Z. Naturforsch. B* **2020**, *75*, 41–50.
[10] J.-Y. Raty, M. Schumacher, P. Golub, V. L. Deringer, C. Gatti, M. Wuttig, *Adv. Mater.* **2019**, *31*, 1806280.
[11] J. Hempelmann, P. C. Müller, P. M. Konze, R. P. Stoffel, S. Steinberg, R. Dronskowski, *Adv. Mater.* **2021**, *33*, 2100163.
[12] P. M. Konze, Dissertation, RWTH Aachen University (Aachen), **2019**.
[13] a) T. H. Lee, S. R. Elliott, *Adv. Mater.* **2020**, *32*, 2000340; b) T. H. Lee, S. R. Elliott, *Phys. Status Solidi RRL* **2021**, *15*, 2000516.
[14] a) G. A. Papoian, R. Hoffmann, *Angew. Chem. Int. Ed.* **2000**, *39*, 2408–2448; *Angew. Chem.* **2000**, *112*, 2500–2544; b) A. Ienco, R. Hoffmann, G. Papoian, *J. Am. Chem. Soc.* **2001**, *123*, 2317–2325; c) G. Papoian, R. Hoffmann, *J. Am. Chem. Soc.* **2001**, *123*, 6600–6608.
[15] Projected force constants are calculated by projecting the force constant tensors received from phononic calculations along individual interatomic vectors to yield a single scalar value for pairwise interaction strength: V. L. Deringer, R. P. Stoffel, M. Wuttig, R. Dronskowski, *Chem. Sci.* **2015**, *6*, 5255–5262.
[16] P. C. Müller, C. Ertural, J. Hempelmann, R. Dronskowski, *J. Phys. Chem. C* **2021**, *125*, 7959–7970.
[17] a) W. V. Glassey, G. A. Papoian, R. Hoffmann, *J. Chem. Phys.* **1999**, *111*, 893–910; b) W. V. Glassey, R. Hoffmann, *J. Phys. Chem. B* **2001**, *105*, 3245–3260.
[18] T. Ohta, *J. Optoelectron. Adv. Mater.* **2001**, *3*, 609–626.
[19] S. A. Semiletov, *Kristallografiya* **1956**, *1*, 403–406.
[20] T. Matsunaga, R. Kojima, N. Yamada, K. Kifune, Y. Kubota, M. Takata, *Appl. Phys. Lett.* **2007**, *90*, 161919.
[21] K. Schubert, H. Fricke, *Z. Naturforsch. A* **1951**, *6*, 781–782.

[22] W. Heitler, F. London, *Z. Phys.* **1927**, *44*, 455–472.
[23] a) F. Hund, *Z. Phys.* **1926**, *36*, 657–674; b) J. P. Lowe, K. A. Peterson, *Quantum Chemistry*, 3rd ed., Elsevier, Academic Press, Burlington, MA, **2006**.
[24] After the molecule has been formed, a proper decomposition of the H_2 electron density may also provide useful chemical-bonding information: R. F. W. Bader, *Atoms in Molecules: A Quantum Theory*, Clarendon Press, Oxford, **1995**.
[25] W. N. Lipscomb, *Science* **1966**, *153*, 373–378.
[26] a) R. E. Rundle, *J. Am. Chem. Soc.* **1947**, *69*, 1327–1331; b) R. E. Rundle, *J. Chem. Phys.* **1949**, *17*, 671–675; c) G. C. Pimentel, *J. Chem. Phys.* **1951**, *19*, 446–448.
[27] A. N. Alexandrova, A. I. Boldyrev, H.-J. Zhai, L.-S. Wang, *J. Phys. Chem. A* **2004**, *108*, 3509–3517.
[28] M. L. Munzarová, R. Hoffmann, *J. Am. Chem. Soc.* **2002**, *124*, 4787–4795.
[29] a) M. Giambiagi, M. S. de Giambiagi, K. C. Mundim, *Struct. Chem.* **1990**, *1*, 423–427; b) A. Sannigrahi, T. Kar, *Chem. Phys. Lett.* **1990**, *173*, 569–572.
[30] a) K. B. Wiberg, *Tetrahedron* **1968**, *24*, 1083–1096; b) I. Mayer, *Chem. Phys. Lett.* **1983**, *97*, 270–274.
[31] a) S. Maintz, V. L. Deringer, A. L. Tchougréeff, R. Dronskowski, *J. Comput. Chem.* **2013**, *34*, 2557–2567; b) S. Maintz, V. L. Deringer, A. L. Tchougréeff, R. Dronskowski, *J. Comput. Chem.* **2016**, *37*, 1030–1035; c) R. Nelson, C. Ertural, J. George, V. L. Deringer, G. Hautier, R. Dronskowski, *J. Comput. Chem.* **2020**, *41*, 1931–1940.
[32] a) P. C. Müller, Master thesis, RWTH Aachen University (Aachen), **2019**; b) P. M. Konze, Private communication.
[33] a) G. Kresse, J. Hafner, *Phys. Rev. B* **1993**, *47*, 558–561; b) G. Kresse, J. Furthmüller, *Comput. Mater. Sci.* **1996**, *6*, 15–50; c) G. Kresse, J. Furthmüller, *Phys. Rev. B* **1996**, *54*, 11169–11186; d) G. Kresse, D. Joubert, *Phys. Rev. B* **1999**, *59*, 1758–1775.
[34] P. E. Blöchl, *Phys. Rev. B* **1994**, *50*, 17953–17979.
[35] G. I. Csonka, J. P. Perdew, A. Ruzsinszky, P. H. T. Philipsen, S. Lebègue, J. Paier, O. A. Vydrov, J. G. Ángyán, *Phys. Rev. B* **2009**, *79*, 155107.
[36] a) S. Grimme, J. Antony, S. Ehrlich, H. Krieg, *J. Chem. Phys.* **2010**, *132*, 154104; b) S. Grimme, S. Ehrlich, L. Goerigk, *J. Comb. Chem.* **2011**, *32*, 1456–1465.
[37] H. J. Monkhorst, J. D. Pack, *Phys. Rev. B* **1976**, *13*, 5188.
[38] P. E. Blöchl, O. Jepsen, O. K. Andersen, *Phys. Rev. B* **1994**, *49*, 16223–16233.
[39] C. Ertural, S. Steinberg, R. Dronskowski, *RSC Adv.* **2019**, *9*, 29821–29830.
[40] R. Hoffmann, H. Fujimoto, J. R. Swenson, C.-C. Wan, *J. Am. Chem. Soc.* **1973**, *95*, 7644–7650.
[41] a) E. J. Skoug, D. T. Morelli, *Phys. Rev. Lett.* **2011**, *107*, 235901; b) M. D. Nielsen, V. Ozolins, J. P. Heremans, *Energy Environ. Sci.* **2013**, *6*, 570–578; c) S. Lee, K. Esfarjani, T. Luo, J. Zhou, Z. Tian, G. Chen, *Nat. Commun.* **2014**, *5*, 3525; d) Y. Yu, M. Cagnoni, O. Cojocaru-Mirédin, M. Wuttig, *Adv. Funct. Mater.* **2020**, *30*, 1904862; e) J.-Y. Raty, C. Gatti, C.-F. Schön, M. Wuttig, *Phys. Status Solidi RRL* **2021**, *15*, 2000534.
[42] A. Togo, I. Tanaka, *Scr. Mater.* **2015**, *108*, 1–5.
[43] L. Zhao, M. Zhi, G. Frenking, *Int. J. Quantum Chem.* **2021**, e26773.
[44] A.-K. U. Michel, M. Wuttig, T. Taubner, *Adv. Opt. Mater.* **2017**, *5*, 1700261.
[45] C. Landis, F. Weinhold, *Inorg. Chem.* **2013**, *52*, 5154–5166.
[46] a) W. P. Anderson, J. K. Burdett, P. T. Czech, *J. Am. Chem. Soc.* **1994**, *116*, 8808–8809; b) L. C. Allen, J. K. Burdett, *Angew. Chem. Int. Ed. Engl.* **1995**, *34*, 2003; *Angew. Chem.* **1995**, *107*, 2157.

Manuscript received: November 19, 2021
Accepted manuscript online: January 10, 2022
Version of record online: February 2, 2022